Core Design Optimization of the Westinghouse Lead Fast Reactor

Nicolas E. Stauff [1], Kyle Ramey [1], Scott Richards [1], Fausto Franceschini [3], Jun Liao [2], Martin Jonson [2], Paolo Ferroni [2]

[1] Argonne National Laboratory, Lemont, IL
[2] Westinghouse Electric Company, Cranberry Township, PA
[3] Westinghouse Electric Company, Mangiarotti, Italy

ABSTRACT

Westinghouse is pursuing an advanced Nuclear Power Plant design based on Lead Fast Reactor (LFR) technology for global commercialization. To achieve an optimal combination of key attributes, such as safety, sustainability, and economic competitiveness, Westinghouse and ANL partnered in developing and applying a formalized core design optimization strategy. An LFR analysis workflow was developed to automate a suite of reactor physics, fuels performance, safety, and economics simulations on a selected LFR concept. The workflow streamlines analysis of a wide range of LFR designs with different dimensions and fuel types to assess their viability and economic performance, significantly reducing human processing time and risks of processing errors. The LFR optimization exercise was defined, resulting in selection of the design constraints (geometric, neutronics, thermo-mechanical, safety, thermal-hydraulics, and economics) and performance metrics researched (minimization of both the fuels LCOE and the first core inventory cost). A total of 14 varied design parameters were considered, including assembly dimensions, coolant temperature, and enrichment distribution throughout the core. The LFR analysis workflow was connected to DAKOTA for sensitivity and optimization analyses. Due to the extremely large size of the potential LFR optimization solution space relative to the computing time required to characterize one LFR solution, a multi-stage optimization approach was proposed to breakdown the problem into several stages with more reasonable sizes. This optimization approach enabled finding various viable core solutions with different cost tradeoffs that were considered by Westinghouse and justify selection of a smaller core with multi-batch 2-year cycle length.

Keywords: Lead Fast Reactor, Optimization, Neutronics, Safety, Fuels performance

1. INTRODUCTION

Westinghouse is pursuing an advanced Nuclear Power Plant design based on Lead Fast Reactor (LFR) technology for global commercialization [1]. To achieve an optimal combination of key attributes, such as safety, sustainability, and economic competitiveness, Westinghouse and ANL partnered in completing a core design optimization. ANL has acquired wide experience in advanced nuclear reactor core design optimization that was applied to ABTR [2], Holos microreactors [3] [4], and initial work was completed on an earlier version of the Westinghouse LFR [5]. Similar efforts are also underway by other groups on LFRs [6] and applying optimization techniques to microreactors [7].

The work summarized in this paper enables effective optimization of an LFR core based on fuel economics performance metrics by building on an extensive workflow, with streamlined execution of neutronics, thermal-hydraulics, fuel rod performance and system analyses, to ensure viability of the core design options being selected against a wide range of design constraints. This paper summarizes the optimization work, with focus on method description while providing a set of representative results obtained.

The baseline LFR model employed for this effort is described in [8], featuring High Assay Low Enriched Uranium (HALEU) UO_2 fuel, with radial and axial layouts shown in Figure 1. The core delivers a power of 950 MWt core and it employs four radial enrichment zones, labeled “inner”, “middle”, “outer”, and “external”, with increasing U-235 enrichment from the inner to the external zone. The fuel assemblies use grid spacers to position the fuel pins within the duct. The fuel features two axial enrichment zones, with top and bottom tip regions at higher U-235 enrichment, and middle zone at lower U-235 enrichment. Two groups of control assemblies, defined as CP (primary control rods) and CS (secondary control rods), are employed to compensate excess reactivity throughout the cycle, while also providing shutdown capabilities independently from the other.

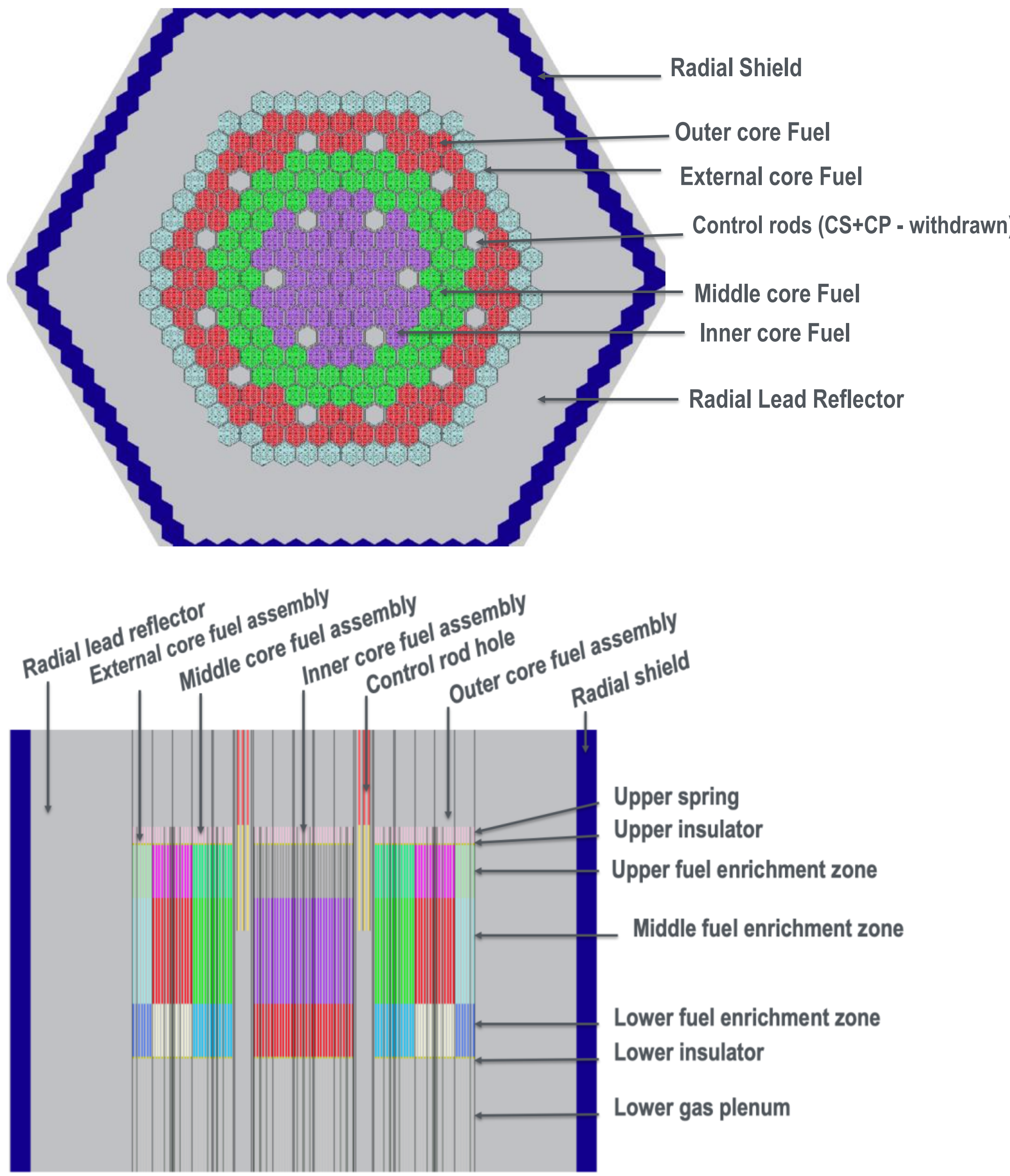

Figure 1. Radial (above) and axial (below) layout of the baseline LFR core.

2. METHODS AND TOOLS

A wide range of calculation tools are used in this project to enable detailed LFR analysis, covering neutronics, thermal-hydraulics, fuel performance, safety analysis, and economics evaluation. WATTS (Workflow and Template Toolkit for Simulation) [9] is used to automate the LFR modeling workflow, connecting tools together with required pre/post-processing capabilities into a combined Python script. WATTS is a generic open-source workflow management tool developed at ANL.

2.1. DAKOTA [10]

The Dakota software maintained by Sandia National Laboratory is an uncertainty quantification and optimization toolkit with over 20 years of development. Dakota provides advanced mathematical methods to vary a code's input parameters and analyze the output results, enabling multi-objective optimization and uncertainty quantification analysis. The core optimization is performed with a multi-objective genetic algorithm (MOGA) and direct physics simulation. MOGA is used based on extensive experience applied at ANL on various previous core design optimization projects.

2.2. PyARC and ARC

The ARC codes have been developed at ANL for over 60 years and some of the components have been used all over the world. The main parts of ARC used for this analysis include MC^2-3 [11] [12], DIF3D [13], GAMSOR [14], PERSENT [15], and DASSH [16]. The ENDF/B-VII.0 nuclear data library [17] is used for this application. For this project, the ARC codes are executed within the PyARC module [18] that handles input pre-processing, workflow execution, and results processing.

The deterministic options used for LFR modeling were selected following the recommendations derived from benchmark analyses performed in [8]. For MC^2-3, cross-sections are processed with a 1D heterogeneous model, to condense them into 33 energy groups. For DIF3D, VARIANT is used as main solver for every calculation, using diffusion P1P0 options.

2.3. SAS for fuels performance and safety analysis [19]

The SAS4A/SASSYS-1 (SAS) code [19] is a multi-physics system analysis code developed for safety evaluation of liquid-metal fast reactors. SAS is actively used at Westinghouse for LFR safety analyses [20]. SAS is used in this project for fuel performance (with DEFORM-4 module) and safety analysis under steady-state and unprotected transient conditions. The DEFORM-4 module of SAS simulates oxide fuel behavior for normal operation and transients and was recently verified and validated on LFR fuel pins.

2.4. Westinghouse economic script

A Python-based methodology to calculate fuel costs and related impact on Levelized Cost of Electricity (LCOE) developed by Westinghouse has been implemented in the workflow [21]. It streamlines calculation of cash flows and timing for each category of plant operation cost and discounts (or escalates) these values back to a reference date, allowing consistent comparison of the economic performance of various core design candidates with respect to operating expenses, and namely fuel expenses, including refueling outage costs.

More specifically, pre-operational, operational and post-operational costs associated with the nuclear fuel cycle are calculated. The pre-operational costs, for HALEU fuel, include purchase of U_3O_8, conversion, enrichment and fabrication. The cost of each uranium commodity component is computed using time dependent values from a price forwarding model. The resulting pre-operational cost is the undepreciated asset value of the fuel prior to operation. The operational phase involves the evaluation of electric generation and the burnup depreciation of the fuel. The fuel asset is depreciated as burnup is accrued up to final discharge (for HALEU fuel and in the current open fuel cycle assumed in the analysis). The time dependent fuel asset value is used to compute the in-core carrying costs required to evaluate the return on the undepreciated fuel asset as it is irradiated through multiple cycles in the reactor. Finally, spent fuel storage and disposal costs for the post-operational phase of the fuel cycle are calculated, and discounted to the reference date.

The fuel LCOE is then calculated by adding pre-operational, operational and post-operational costs divided by the amount of energy produced (discounted by inflation) by the fuel during its residence time in the reactor. Outage expenses, which vary for the various scenarios evaluated as a result of the different fuel management schemes and time intervals between refueling, are also accounted for in terms of maintenance personnel cost and replacement power that needs to be purchased during outages. The outage length accounts for the wait time to safely dry-lift fuel assemblies, which depends on their decay heat and geometry, and is calculated as part of the workflow developed for this work, as discussed in Section 4. In this way, fuel cycle and outage expenses for various scenarios can be calculated over a consistent period of time (e.g. the reactor lifetime) and compared as part of determining economically optimal candidates.

3. OPTIMIZATION METHOD

The overall design analysis approach applied to the Westinghouse LFR is summarized in Figure 2.

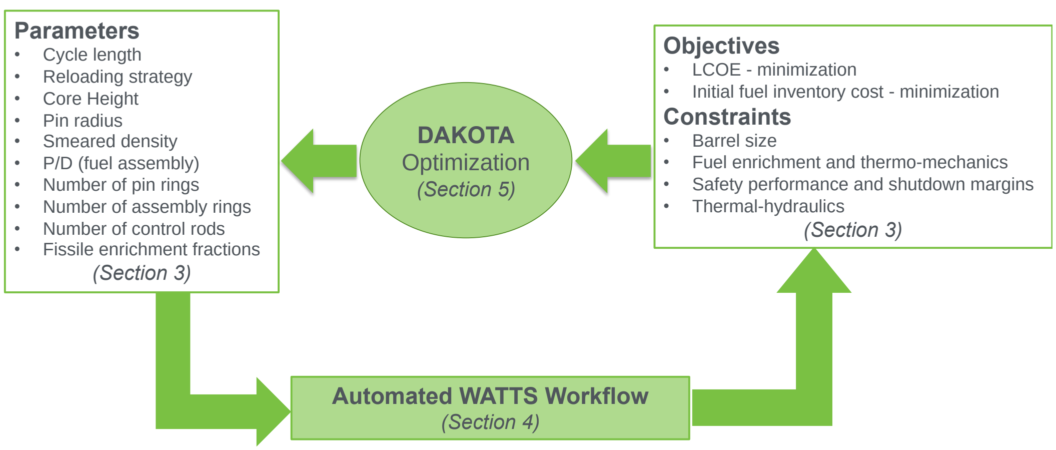

Figure 2. Summary of LFR design approach.

There are two objective functions that have been selected to be optimized (e.g. minimized) for the LFR core:

- LCOE ($/MWh). Note that for discriminating economic performance of the various core designs, only fuel cycle cost plus outage expenses needed to be accounted for, as the remaining components of the overall plant LCOE is not affected by the specific core design solution being proposed (within the assumed boundary condition of this analysis of a fixed barrel size). This metric is linked to many other performance metrics such as fuel burnup, outage length, and thermal efficiency, which may change for the various core designs analyzed according to the core-average lead outlet temperature that each can support.
- Cost of initial (startup) core fuel inventory (M$). This metric is linked to the total mass of fuel and fissile content in the core needed to reach criticality throughout the first cycle. While for single-batch designs it was possible to accurately calculate this performance metric, as it coincides with the cost of reloads, for multi-batch designs first core cost was calculated in a conservative fashion multiplying the cost of a reload at the equilibrium cycle, by the number of batches.

3.1. Design Constraints

The design constraints selected for this optimization exercise are summarized in Table 1. These are "hard" constraints, meaning that a core solution that fails to meet one of these requirements during the optimization workflow will be disregarded. Note that specifics relating to calculation steps will be discussed in detail later in section 4.

Table 1. Summary of core design constraints.

Constraint	*Unit*	*Limit*	*Calc Step*
Geometry / Neutronics			
Max. core barrel radius	m	1.93 (cold)	1
Max. fuel assembly weight	MT	3	1
Max. U-235 enrichment	w%	19.75	2
Min. control margin	$	0	4
Min. safety margin	$	0	4
Thermo-mechanical			
Max. clad thermal creep (steady-state)	%	0.2	10
Max. clad strain (steady-state)	%	2	10
Max. CDF* (steady-state)	%	0.05	10
Safety			
Max. rod ejection worth	$	1	4
Max. RV temperature (transient)	°C	750	10
Max. CDF* (transient)	%	0.1	10
Max. fuel temp (transient)	°C	2865	10
Thermal Hydraulics			
Max. fuel temp (steady-state)	°C	2765	10
Max. coolant velocity	m/s	2	
Economics			
First core cost	Normalized**	1.25	8

* CDF: Cumulative creep Damage Fraction

** refer to Figure 3

3.2. Varied Parameters

The core design parameters to be varied during the optimization workflow were identified (as listed in Figure 2), together with their range of interest. There are 15 different variables, some with a range of discrete or continuous values, others with Boolean-type options. This relatively extensive list of parameters has then been reduced after sensitivity analysis performed as part of various rounds of optimization. From these input variables, the relevant LFR design dimensions are being derived and used to setup the different PyARC and SAS models. An initial sensitivity analysis completed showed that only about 7% of the cases were passing all design constraints, the rest failing in Step #0 (due to the maximum core radius constraint), #1 (due to the maximum U-235 enrichment constraint), #5 (due to excessive coolant velocity), and #10 (due to exceeding the CDF limits in steady-state and ULOSSP transients).

For the optimization calculation, the main parameters to adjust are the number of initial samples (first generation) and maximum number of samples allowed. An initial good scan of the space ensures not to miss areas of interest and convergence to a local optimum solution. For the LFR workflow analysis, the size of the problem had to be constrained accounting for the time required to converge one simulation using the available computing resources. For practicality, a maximum number of 3,000 simulations was targeted so that completion of an optimization round could be performed within 30 days. The full range of combinations to sample for the LFR core design optimization is extremely aggressive with more than 10^{12} potential options to consider. To be able to ensure full coverage of the design space, one would need around half a million simulations of the LFR workflow, which is unrealistic under current computing constraints. Using a small number of initial simulations will most likely lead to not properly investigating the full design space and result in convergence to local minima. Expert judgement informed from the early experience performing many initial simulations was used to reduce the size of the problem through prioritization of parameters, breaking down the problem into two successive smaller stages:

- First Stage: the initial stage focuses on wide range analysis across the geometry space. However, many variables were fixed, due to their expected lower impact on the LFR key performance metrics, using reference value as fixed points. In this case, the cycle length is researched to target material dose close to (but less than) the "soft" 120 DPA cladding limit as higher DPA levels are expected to fail "hard" CDF limits set for this core design optimization effort. Thanks to this judicious choice, the size of the solution space in this first stage could be significantly reduced, resulting in an initial population of 300 cases.
- Second Stage: The second stage consists in refining the optimization of the preferred solution among the best candidates obtained in Stage 1. Accordingly, most of the parameters varied in Stage 1 are fixed in Stage 2, or their ranges are reduced. New sets of parameters (such as the enrichment modification factors across different axial and radial core regions) are varied around the value from the Stage 1 solution to attain further performance improvements. Once again, the space size could be kept at a reasonable size with this approach, allowing to select an initial population of 300 cases also for Stage 2 optimization simulations.

4. OVERVIEW OF THE LFR ANALYSIS WORKFLOW

The LFR optimization relies on an automated LFR analysis workflow that takes about three hours to complete (if design constraints are not violated sooner) using one CPU for a single candidate core. This allows thorough assessment of the viability and performance of a design candidate, using traditional fidelity modeling capabilities.

This comprehensive 10-step workflow is summarized in Table 2, showing the codes employed in each step together with key tasks achieved, output from the analysis and the approximate CPU time required to perform it. While one workflow calculation typically requires running all the steps consecutively, the workflow stops whenever it detects a failed hard constraint, helping to save computation time on unviable cases.

Table 2. Summary of multi-step WATTS workflow developed for LFR analysis.

Step	*Codes*	*Task*	*Output*	*CPU Time (min)*
1	Python	Pre-processing of core dimensions	Cold/Hot dimensions Geometric constraints	0
2	MC^2-3 REBUS	Initial XS calculation and enrichment search calculation	Reloading enrichment and BOEC composition Cycle length adjusted to stay below 120DPA *	25
3	DIF3D	S-curve calculations	S-curve	3
4	DIF3D	Shutdown margin calculations	Shutdown margin requirements	5
5	REBUS ORIGEN	Depletion with CR at critical position	Critical rods position Decay heat curve	20

6	GAMSOR	Gamma heating (BOL/EOL)	Power distribution Average flow rate in different regions	25
7**	REBUS GAMSOR DASSH	Sub-channel calculation (BOL/EOL)	Pressure drop Peak pin/cladding temperature constraints	60
8	Economics script	Liftoff time, thermal efficiency, and fuel cost calculations	Outage duration LCOE & Inventory cost	0
9	MC^2-3 DIF3D PERSENT	Perturbation calculations (EOL)	Reactivity coefficients for SAS	60
10	SAS	Fuels Performance Safety transients calculations	Steady-state fuels performance Transients (PLOSSP, ULOSSP, UTOP) performance	30

* This option to adjust the cycle length to attempt to reach close to 120 DPA is used in early optimization analyses to try to converge earlier to more economic optimum solutions.

** This sub-channel calculation step is skipped during the optimization workflow as its results are currently not used as hard constraints in the optimization, relying instead on SAS results from step #10.

5. OPTIMIZATION RESULTS

The first stage of the optimization was completed over 25-30 generations for a total of ~3000 solutions considered. The results of this optimization are shown in Figure 3, with normalized LCOE and core inventory values with respect to their values at the start of the optimization. Each point shown on this figure represents a fully characterized LFR design, where grey points failed at least one constraint, and blue/purple points met all constraints. Lighter blue points were considered in the earlier optimization generations, while purple points were found in later generations. This color transition helps show convergence of the optimization algorithms toward viable solutions with lowest fuel cycle LCOE and initial core fuel inventory costs.

The two objective functions selected for this study (fuel LCOE and core inventory cost) evinced opposite optimization trends. This is attributable to the fact that a larger fuel inventory typically entails a larger core size, with fewer neutron leakages, lower enrichment and higher conversion ratio, and thereby improved initial fissile use which, even more so for HALEU cores, is a predominant factor in achieving better fuel economics; on the other hand, a larger fuel inventory negatively impacts first core costs. A larger fuel inventory also favors longer intervals between refueling, with reduced impact of the refueling outage on overall operating expenses, with further benefit on outage schedule from the lower fuel decay heat (from the reduced core power density) and wait time for fuel dry-lift. On the other hand, long cycles also entail higher in-core carrying charges (and relative impact on fuel LCOE) from the long fuel residence time and large reload costs, which eventually caps the achievable improvements in fuel LCOE.

Multi-batch fuel management is preferred as enabling smaller fuel inventory, while favoring improved fissile use with respect to single-batch fuel management. Lower LCOE can also be obtained for solutions with higher operating temperature and thus thermal efficiency, which are more easily achieved reducing power density at the expense of higher core inventory and associated cost. A higher discharge burnup (still within the 120 DPA limit assumed) also enable lowering fuel LCOE. As a result of the many (and often competing) factors at play with respect to the set optimization goals, there are many design options that may enable reaching different types of optimal solutions. The optimization converges to a Pareto Front, with three groups of solutions identified:

- Lower LCOE/Higher fuel inventory cost (upper region of the plot)
- Medium values for LCOE and fuel inventory costs (center of the plot)

- Higher LCOE/Lower fuel inventory cost (bottom/right of the plot)

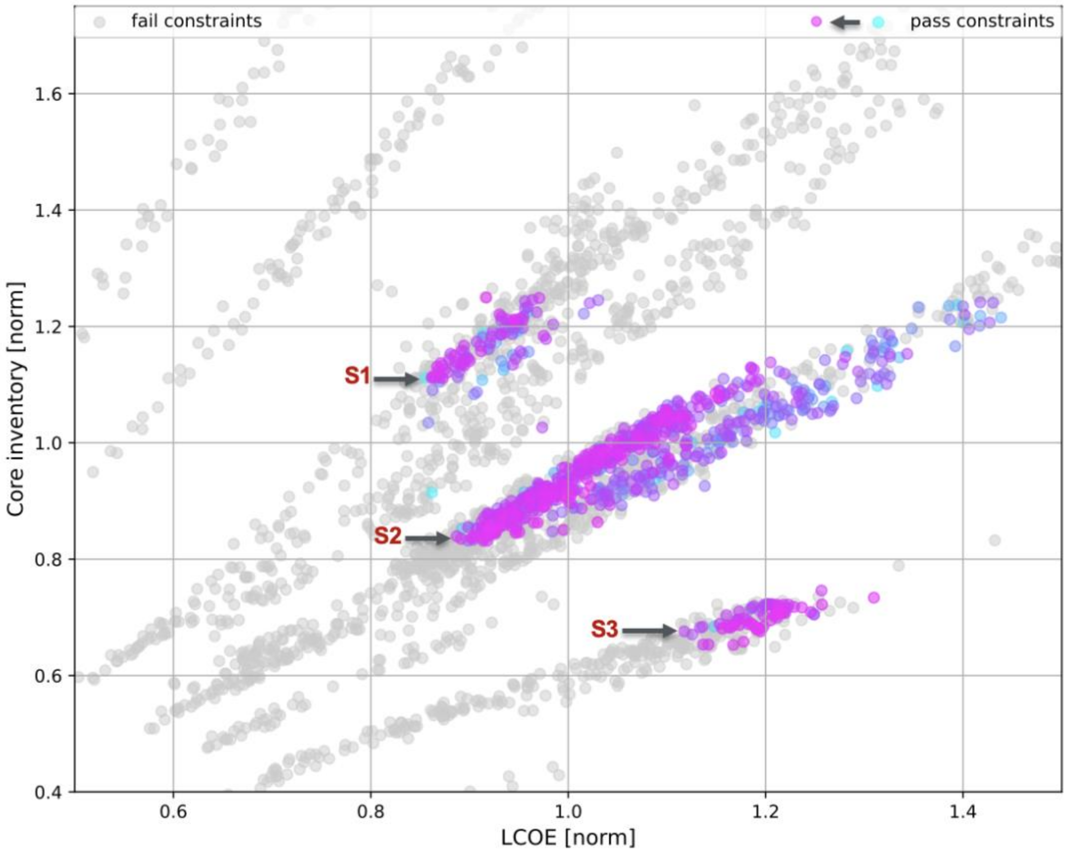

Figure 3. Optimization results for Stage 1 of the LFR with UO_2 – blue-purple pass constraints / grey fail at least one constraint.

From these three groups, optimal core design candidates can be extracted from the Pareto Front, such as "S1" (representative of lower LCOE/higher fuel inventory cost solutions), "S2" (medium LCOE and fuel inventory cost) "S3" (higher LCOE and lower fuel inventory costs) as shown in Figure 3. These solutions feature different combinations of design options and fuel management schemes to achieve the various optimization objectives. For instance, S1 features a relatively high core inventory with a 2-batch refueling scheme, a 4-year cycle length. On the other hand, S3 features about half the fuel inventory compared to S1, relying on same fuel management but higher U-235 enrichment to achieve half the cycle length of S1.

Outside of these three main groups, a few outliers are still observed showing potentially interesting local minimum solutions. From these results, it is concluded that despite the judicious effort performed to reduce the size of the space, more work is needed to enable a fully converged optimization by increasing the number of initial solutions, and avoid reducing too quickly the number of evaluations for each new population.

The optimum candidates can then be further optimized in a second stage by tuning the enrichment modification factors and cladding thickness to gain margins to different design constraints that are leveraged to increase coolant outlet temperature. This was demonstrated for one of the optimal candidates, where thanks to the second state of optimization it has been possible to raise the core outlet temperature by 25 ºC with respect to the first-stage optimal design candidate (with resulting improvement in efficiency and LCOE) while reducing the fuel active length (thereby further reducing fuel inventory cost). Detailed core performance characteristics including results from the safety analyses will be covered in future publications.

6. CONCLUSIONS

A formal approach was developed to support design and optimization of the Westinghouse LFR core. It relies on a comprehensive and efficient analysis workflow that performs a suite of reactor physics, fuel performance, safety, and economics simulations for a selected LFR concept. This enables streamlined analyses of a wide range of LFR design configurations to efficiently assess their viability and economic performance, significantly reducing human processing time and risks of processing errors. The LFR analysis workflow was connected to DAKOTA for optimization analysis aiming at optimal fuel economic performance while meeting a wide range of design constraints (geometric, neutronics, thermo-mechanical, safety, thermal-hydraulics, and economics).

This optimization approach enabled finding various viable core solutions that were considered by Westinghouse, with different LCOE versus first inventory cost tradeoff, enabling the selection of an optimum LFR solution with HALEU UO_2 fuel. Follow-up work will focus on optimization of MOX- and UN-fueled LFR cores.

The developed core design optimization approach enables reallocation of human/machine efforts for effective reactor design and analysis: after a front-end investment in workflow development, human effort in modeling different physics of early-stage core design solutions can be reduced through automation and concentrated in making strategic decisions.

ACKNOWLEDGMENTS

Argonne National Laboratory's work was supported by U.S. Department of Energy (DOE) under Contract number DE-AC02-06CH11357. The direction and support of the U.S. DOE Office of Nuclear Energy is greatly appreciated. The work summarized in this report was supported by Westinghouse.

REFERENCES

[1] P. Ferroni, «The Westinghouse Lead Fast Reactor: design overview and update on development activities,» de *ICAPP*, Las Vegas, 2024.

[2] K. Zeng, N. Stauff, J. Hou y T. K. Kim, «Development of multi-objective core optimization framework and application to sodium-cooled fast test reactors,» *Progress in Nuclear Energy,* vol. 120, 2020.

[3] A. Kasam-Griffith, N. Stauff, Y. Miao, S. Bhattacharya y C. Filippone, «Design Optimization of the Holos-Mono Microreactor Concept,» de *Proceedings of the ANS Winter*, 2022.

[4] N. E. Stauff, C. H. Lee, A. Wells y C. Filippone, «Design Optimization of the Holos-Quad Micro-Reactor Concept,» de *PHYSOR*, 2020.

[5] T. K. Kim, N. Stauff, C. Stansbury, A. Levinsky y F. Franceschini, «Long Core Life Options for the Westinghouse LFR,» de *Global*, Seattle, 2019.

[6] K. A. Al-Dawood y S. P. Palmtag, «LMFR Design and Optimization Methodology,» de *PHYSOR*, Pittsburgh, 2022.

[7] E. Popov, R. Archibald, B. Hiscox y V. Sobes, «Artificial intelligence-driven thermal design for additively manufactured reactor cores,» *Nuclear Engineering and Design,* nº 395, 2022.

[8] N. Stauff, A. Abdelhameed, A. Levinsky y F. Franceschini, «Neutronic Benchmark on the Westinghouse Lead Fast Reactor,» de *PHYSOR*, San Francisco, 2024.

[9] P. K. Romano, N. E. Stauff, Z. J. Ooi, Y. Miao, A. Lund y L. Zou, «WATTS: Workflow and template toolkit for simulation,» *Journal of Open Source Software,* 2022.

[10] B. Adams, et al., «Dakota, A Multilevel Parallel Object-Oriented Framework for Design Optimization, Parameter Estimation, Uncertainty Quantification, and Sensitivity Analysis: Version 6.5 User's Manual,» Sandia National Laboratory, Albuquerque, NM, U.S.A., 2016.

[11] C. Lee y W. Yang, «MC2-3: Multigroup Cross Section Generation Code for Fast Reactor Analysis,» Argonne National Laboratory, Lemont, IL, USA, 2013.

[12] C. Lee y N. Stauff, «Improved Reactivity Worth Estimation of MC2-3/DIF3D in Fast Reactor Analysis,» de *ANS meeting*, San Antonio, 2015.

[13] K. L. Derstine, «DIF3D: A Code to Solve One-, Two-, and Three-Dimensional Finite Difference Diffusion Theory Problems,» ANL-82-64, Argonne National Laboratory, Lemont, IL, USA, 1984.

[14] M. A. Smith y C. Lee, «GAMSOR: Gamma Source Preparation and DIF3D Flux Solution,» Argonne National Laboratory, ANL/NE-16/50 Rev. 1.0, 2017.

[15] M. A. Smith, «Perturbation and Sensitivity Tool Based on the VARIANT Option of DIF3D,» de *ANS Transaction*, San Diego, 2012.

[16] M. Atz, M. A. Smith y F. Heidet, «DASSH software for ducted assembly thermal hydraulics calculations – overview and benchmark,» de *Transactions of the American Nuclear Society 123 pp. 1673-1676*, 2020.

[17] M. B. Chadwick, «ENDF/B-VII.0: Next Generation Evaluated Nuclear Data Library for Nuclear Science and Technology,» *Nuclear Data Sheets,* vol. 107, nº 12, p. 2931–3060, 2006.

[18] N. Stauff, «Integration of PyARC/Workbench with New Fast Reactor Modeling and Simulation Capabilities,» ANL/NEAMS-20/2, 2020.

[19] T. H. Fanning, A. J. Brunett y L. Ibarra, «The SAS4A/SASSYS-1 Version 5.6 Safety Analyis Code System,» ANL/NSE-SAS/5.6, 2022.

[20] J. Liao y e. al., «Applicability enhancement of SAS4A/SASSYS-1 computer code to Lead Fast Reactor systems,» de *IAEA Technical Meeting on state-of-the-art thermal-hydraulics of fast reactors*, Camugnano, Italy, 2022.

[21] D. L. Stucker, J. Norrell, H. Lam y F. Franceschini, «Levelized Cost of Electricity Evaluation Methodology Applied to High-Burnup 18 and 24-Month Fuel Cycles,» de *ICONE-28*, 2021.